Effect of Electromagnetic Field on Microstructure and Properties of Cu-Cr-Co-Si Alloy

Xinglong Sun [1], Jinchuan Jie [1*], Tingju Li [2]

[1] Key Laboratory of Solidification Control and Digital Preparation Technology (Liaoning Province), School of Materials Science and Engineering, Dalian University of Technology, Dalian 116024, China
[2] Laboratory of Special Processing of Raw Materials, School of Materials Science and Engineering, Dalian University of Technology, Dalian 116024, China

Corresponding author: jiejc@dlut.edu.cn

Abstract

The Cu-Cr-Co-Si alloy is a newly designed copper alloy with high mechanical properties and a proper electrical conductivity. The intermediate frequency electromagnetic field was applied during the solidification process. The results showed that the grain size remarkably refined with the application of electromagnetic field, the structure of the as-cast Cu-1Cr-1Co-0.2Si alloy transformed from coarse grain to homogeneous equiaxed grain due to the electromagnetic force. The microhardness and tensile strength of the alloy with the electromagnetic field intensity of 10 mT increased by 27.4% and 14.9% respectively compared with as-cast condition after solid solution and aging treatment. While, the electrical conductivity of the ingots with electromagnetic field is 53.1% IACS, which is slightly lower than that of the as-cast condition.

Keywords: Cu-Cr-Co-Si alloy, Electromagnetic field, Microstructure, Hardness, Tensile strength, Electrical conductivity.

Introduction

Cu-Cr alloys are the most potential alloys that meet comprehensive performance of high strength and high electrical conductivity, which have been widely used in industrial applications such as lead frames, railway contact wires, connectors, heat transfer elements and resistance welding electrode materials[1-3]. Alloying has been proved to be an effectively method to improve the mechanical properties with a slightly decrease of electrical conductivity[4-6]. Hence, a new type Cu-Cr alloy with Co and Si additions was designed. The high strength is attribute to the precipitation and particle dispersion strengthening mechanisms, while the electrical conductivity is decreased due to solute atom that dissolve into the Cu matrix. The main structural requirement of the Cu-Cr-Co-Si alloy is the homogeneous distribution of refined precipitation. Hence, a long time of homogenizing annealing is needed to eliminate the segregation of solutes ahead of solution treatment[7,8]. However, being in high temperature for a long time can result in a severe grain coarsening[9,10]. Thus, the use of magnetic field is a promising topic in the fabrication of materials.

Magnetic field has been successfully applied into the improvement of the solidification structure[11]. Extensive researches in the past demonstrated that the melt acted by appropriate magnetic field has the advantages of refining solidification structure and reducing segregation[12,13]. Therefore, electromagnetic field is considered to apply into the solidification of Cu-Cr-Co-Si alloy to improve the structure and to reduce the segregation of solutes, which helps to shorten the homogenizing annealing. This study investigated the influence of magnetic field on the microstructure, precipitate distribution and properties of Cu-Cr-Co-Si alloy.

Experimental Procedures

The Cu-1Cr-1Co-0.2Si alloy was prepared in a 5 kg intermediate frequency induction furnace with electrolytic copper (99.97 wt.%), pure chromium (99.8 wt.%), pure cobalt (99.9 wt.%) and pure silicon (99.9 wt.%). At first, the electrolytic copper, cobalt, and silicon were melted in the furnace. Pure chromium was added to the melt as the temperature reached 1300 ^{o}C. Then the temperature was held at 1300 ^{o}C for 10 min to ensure the adequately melting of

Cr, Co and Si elements. Finally, the melt was poured into the mold with a diameter of 60 mm, the magnetic field was imposed during the solidification process. Fig. 1 is the schematics of the magnetic field experiment instruments. The magnetic flux density, *B*, used in this experiment was 10 mT. The Cu-1Cr-1Co-0.2Si alloy solidified without magnetic field was prepared as a comparison. The ingots were solution treated at 990 ℃

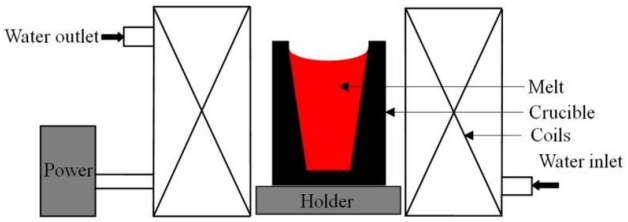

Fig. 1 The schematics of the electromagnetic field experiment instrument.

The microstructures were observed by optical microscope (OM, MEF4, Leica company, Solms, Germany) and field emission scanning electron microscope (FESEM, SUPRA55, Carl Zeiss company, Oberkochen, Germany). Mechanical properties were tested by a universal electronic tensile-testing machine. At least three standard tensile bars of φ10mm were tested for each sample. All tensile tests were performed at room temperature with a strain rate of 1 mm/min. The microhardness was measured using a Vickers hardness tester under 300 g loads maintaining 15s. The electrical conductivity was measured using a D60K conductivity measuring instrument, which is characterized by International Annealed Copper Standard (% IACS).

Results

Macrostructures and microstructures.

Fig. 2 shows the macrostructures and SEM images of Cu-Cr-Co-Si alloy with and without magnetic field. It can be seen that the macrostructure of as-cast Cu-Cr-Co-Si alloy without magnetic field are mainly coarse columnar grains. With the application of the magnetic field, the solidification structure tends to homogeneous equiaxed grains and the average grain size refined from 3000 μm to 750 μm (Fig. 2a-b). Two kind of newly formed phases are formed during the melting and solidification (Fig. 2c-d). The EDS analysis confirms the phase with gray color and a large size is $Cr_{15}Co_9Si_6$, while the other phase with white and a small size is Co_2Si. Meanwhile, the number of the particles distributes more uniform with the application of magnetic field.

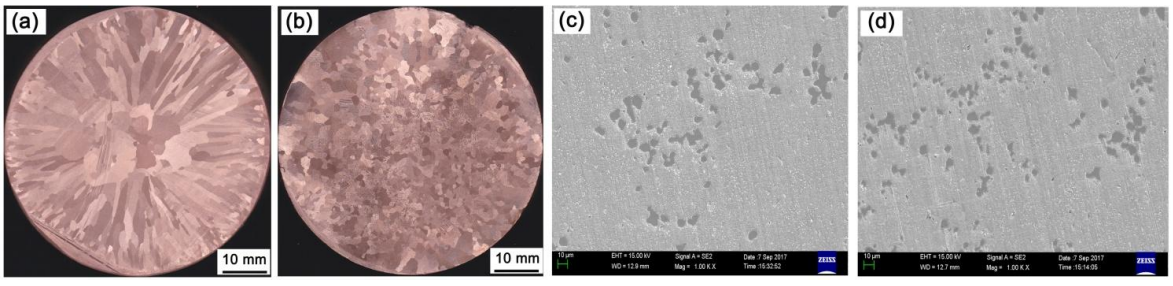

Fig.2 Macrostructures and SEM images of as-cast Cu-1Cr-1Co-0.2Si alloy with and without electromagnetic field: (a) and (c) *B*=0; (b) and (d) *B*=10 mT

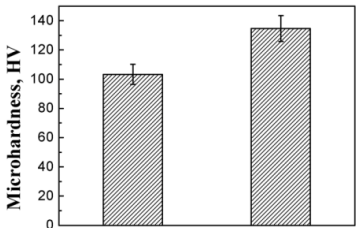

Fig. 3 Microhardness comparsion of the Cu-1Cr-1Co-0.2Si alloy with and without electromagnetic field.

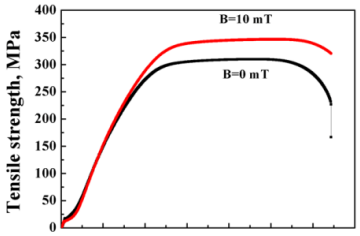

Fig. 4 Stress-strain curves of the Cu-1Cr-1Co-0.2Si alloy with and without electromagnetic field.

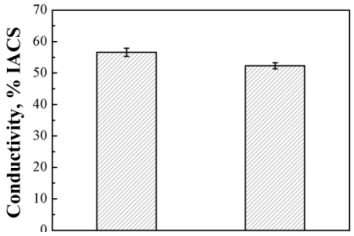

Fig. 5 Electrical conductivity comparsion of the Cu-1Cr-1Co-0.2Si alloy with and without electromagnetic field.

Properties

Fig. 3 presents the microhardness comparsion of the Cu-1Cr-1Co-0.2Si alloy with and without magnetic field. It can be seen that the average values of microhardness under magnetic field *B*=0 and *B*=10 mT are 103.3 HV and 131.6 HV, respectively. With the application of magnetic field, the microhardness increases by 27.4 %. Fig. 4 exhibits the stress-strain curves of the Cu-1Cr-1Co-0.2Si alloy with and without magnetic field. The tensile strength of Cu-1Cr-1Co-0.2Si alloy solidified under magnetic field *B*=0 and *B*=10 mT are 306.4 MPa and 352.1 MPa, respectively. With the application of magnetic field, there is an evident increment in tensile strength and elongation. The increment of tensile strength is in correspondence with the particle distribution are shown in Fig. 2c-d. The slight improvement of elongation under electromagnetic field is due to the grain refinement as shown in Fig. 2a-b. Since the macrostructure of Cu-1Cr-1Co-0.2Si alloy transforms to refined equiaxed grains under the effect of magnetic field, the difference between deformation within the grain and grain boundaries grows less. Thus total deformation becomes more uniform under the action of external force. The electrical conductivity comparsion of Cu-1Cr-1Co-0.2Si alloy with and without electromagnetic field is shown in Fig. 5. The average values of electrical conductivity under electromagnetic field *B*=0 and *B*=10 mT are 57.6 %IACS and 53.1 %IACS, respectively. With the application of electromagnetic field, there is a light decrease in electrical conductivity, which is due to the increase of interface scattering.

Discussion

The effect of magnetic field on grain refinement.

The coils create a rotating magnetic field when alternating current is imposed. To the melt, under the effect of magnetic field, generates an induced eddy current in turn. As a result, the melt is subjected to a Lorentz force under the common action of induced eddy current and rotating magnetic field, which can be expressed as follows [14]:

$$F = J \times B \tag{1}$$

where *J* is the induced eddy current, and *B* is the magnetic flux density.

The low temperature melt near the edge of graphite is taken to the center by the electromagnetic body force, and the temperature gradient in the melt reduces. The compulsive convection caused by magnetic field generates shearing force, and plenty of dendrites are broken off [15, 16]. The flow transports these fragments from the interdendritic spacing to the region ahead of the solidification front. In this area, the fragments offer cores for nucleation. Since the nucleation rate increases and temperature field becomes homogeneous, the solidification structure transfers from big columnar dendrites to refined equiaxed grains over the cross–section.

The effect of magnetic field on the properties.

Particle strengthening occurs due to the Orowan dislocation bypass mechanism. This mechanism comprises a dislocation bow–cut and bypassing between un-deformable particles, leaving a dislocation loop around the particles. According to the Orowan strengthening model, the strength increment can be calculated as follows[17,18]:

$$\Delta\sigma_{Or} = 0.84\frac{MGb}{2\pi r\sqrt{1-\nu}\left(\sqrt{\frac{3\pi}{2f}}-\pi/4\right)}\ln\left(\frac{r}{4b}\right) \quad (2)$$

where M is the Taylor factor for the fcc copper matrix, b is the Burgers vector, G is the shear modulus of the matrix, υ is the Poisson's ratio of the copper matrix, r and f represent the average radius and volume fraction of the particle precipitates, respectively. With the application of magnetic field, the precipitation particles are refined and their amount increases, resulting in an improvement of tensile strength and microhardness.

The resistivity of copper matrix can be partitioned into the contribution of four main scattering mechanisms [19]:

$$1/\sigma_{alloy} = \rho_{alloy} = \rho_{imp} + \rho_{def} + \rho_{int} + \rho_{pho} \quad (3)$$

where ρ_{pho} is the resistivity contribution from phonon scattering, ρ_{def} is the dislocation scattering, ρ_{int} is the interface scattering, and ρ_{imp} is the impurity scattering. The Alloy with and without magnetic field have similar values of ρ_{imp}, ρ_{def} and ρ_{pho}. Since the amount of precipitate increases with the application of magnetic field, the more interface produced between the Cu matrix and the particles increases the ρ_{int}. Thus, with the application of magnetic field, the total resistivity of aged Cu-1Cr-1Co-0.2Si alloy is increased and the electrical conductivity is reduced.

Summary

(1) The macrostructure of Cu-1Cr-1Co-0.2Si alloy transform from coarse columnar grains to refined equiaxed grains with the application of magnetic field.

(2) The microhardness and tensile strength of aged Cu-1Cr-1Co-0.2Si alloy increases with increasing the magnetic field.

(3) The electrical conductivity of aged Cu-1Cr-1Co-0.2Si alloy exhibits a slight decrease with increasing magnetic field.

Acknowledgement

The authors gratefully acknowledge the supports of National Key Research and Development Program of China (Nos. 2016YFB0301303, 2017YFA0403800).

References

1. Q.J. Wang, Z.Z. Du, L. Luo, W. Wang: J. Alloy Compound. Vol.526 (2012), 39–44.
2. C.D. Xia, W. Zhang, Z.Y. Kang: Mater. Sci. Eng. A.Vol.538 (2012), 295–301.
3. M. Bizjak, B. Karpe, J. Kovac: Appl. Surf. Sci Vol.277 (2013), 83–87.
4. J.H. Su, Q.M. Dong, P. Liu, H.J. Li, and B.X. Kang: Mater. Sci. Eng. A. Vol.392(2005), 422.
5. S.J. Sun, S. Sakai, H.G. Suzuki. Mater. Sci. Eng. A. Vol.303 (2000), 187–196.
6. J.E. Bailey and P.B. Hirsch: Philos. Mag. Vol.5 (1960), 485.
7. S.G. Jia, X.M. Ning, P. Liu, M.S. Zheng, G.S. Zhou, Met. Mater. Int. 15 (2009) 555–558.
8. S.G. Jia, M.S. Zheng, P. Liu, F.Z. Ren, B.H. Tian, G.S. Zhou and H.F. Lou: Mater. Sci. Eng. A Vol. 419 (2006), p. 8
9. T.H. Kim and J.K. Park: Mater. Sci. Technol. Vol. 29 (2013), p. 1414
10. M. Akiyama, Y. Neishi and Y. Adachi: Eng. Computation Vol. 20 (2003), p. 499
11. X. Zhang, D.L. Wang, S.X. Zhang, Y.W. Ma, W.S. Yang, Y. Wang, S: J. Magn. Magn. Mater. Vol. 322 (2010), p. 302
12. T.J. Li, Z.Q. Cao, J.Z. Jin, and Z.F. Zhang: Mater. Trans. JIM Vol. 42 (2001), p. 281
13. W.Z. Jin, F.D. Bai, T.J. Li, and G.M. Yin: Mater. Lett. Vol. 62 (2008), p. 1585
14. C. Vives: Metall. Mater. Trans. B. Vol.20 (1989), p. 623
15. S. Eckert, P. A. Nikrityuk, B. Willers, D. Rabiger, N: Eur. Phys. J. Special Topics Vol. 220 (2013), p. 123
16. J. Stiller, K. Koal, W.E. Nagel and J. Pal, A. Cramer: Eur. Phys. J. Special Topics Vol. 220(2013), p. 111
17. J.L. Xu and S.X. Jin: Plasma Physics, Atom Energy Press, Beijing (1998).
18. J. Li, T. Wang, J. Xu, Z. Yan, J. Sun, J. Xu, Z. Cao and T. Li: Mater. Sci. Technol. Vol. 27 (2011), p. 676
19. L. Qu, E.G. Wang, K. Han, X.W. Zuo: J. Appl. Phys. Vol.113(2013), 173708.